CHAPTER 3
Fault Selection

ANALYTIC REDUNDANCY is an approach to health monitoring that compares dissimilar instruments using a detailed model of the system dynamics. Therefore, to detect a fault in a given sensor, there must be a dynamic relationship between the sensor and other sensors or actuators. That is, the information provided by a monitored sensor must, in some form, also be provided by other sensors. Analytic redundancy also can be used to effectively monitor the health of system actuators and even the dynamic behavior of the system itself. But, as with sensors, if some part of the vehicle is to be monitored for proper operation, then that part has to produce some observable dynamic effect.

In automated vehicles, these requirements preclude monitoring nonredundant sensors such as obstacle detection or lane position sensors. The information provided by a radar or infrared sensor designed to detect objects in the vehicle's path has no dynamic correlation with other sensors on the vehicle. A sensor that detects the vehicle's position in a lane is the only sensor that can provide this information. Actuators that do no observable action

are also difficult to monitor. For example, the health of a power window actuator is easily monitored by the driver. But, unless specialized sensors are installed, no other part of the car is affected by the operation of this actuator and there is no analytic redundancy.

Before describing how faults are modeled, it is necessary to describe how a fault detection filter works. Most of the details are left to Appendix A. For a thorough background, several references are available, a few of which are (Douglas 1993), (White and Speyer 1987) and (Massoumnia 1986). Consider a linear time-invariant system with q failure modes and no disturbances or sensor noise

$$\dot{x} = Ax + Bu + \sum_{i=1}^{q} F_i m_i \tag{3.1a}$$

$$y = Cx + Du \tag{3.1b}$$

The system variables x, u, y and the m_i belong to real vector spaces and the system maps A, B, C, D and the F_i are of compatible dimensions. Assume that the input u and the output y both are known. The F_i are the failure signatures. They are known and fixed and model the directional characteristics of the faults. The m_i are the failure modes and model the unknown time-varying amplitude of faults. The m_i do not have to be scalar values.

A fault detection filter is a linear observer that, like any other linear observer, forms a residual process sensitive to unknown inputs. Consider a full-order observer with dynamics and residual

$$\dot{\hat{x}} = (A + LC)\hat{x} + Bu - Ly \tag{3.2a}$$

$$r = C\hat{x} + Du - y \tag{3.2b}$$

Form the state estimation error $e = \hat{x} - x$ and the dynamics and residual are

$$\dot{e} = (A + LC)e - \sum_{i=1}^{q} F_i m_i$$

$$r = Ce$$

In steady-state, the residual is driven by the faults when they are present. If the system is (C, A) observable, and the observer dynamics are stable, then in steady-state and in the

absence of disturbances and modeling errors, the residual r is nonzero only if a fault has occurred, that is, if some m_i is nonzero. Furthermore, when a fault does occur, the residual is nonzero except in certain theoretically relevant but physically unrealistic situations. This means that any stable observer can detect the presence of a fault. Simply monitor the residual and when it is nonzero a fault has occurred.

In addition to detecting a fault, a fault detection filter provides information to determine which fault has occurred. An observer such as (3.2) becomes a fault detection filter when the observer gain L is chosen so that the residual has certain directional properties that immediately identify the fault. The gain is chosen to partition the residual space where each partition is uniquely associated with one of the design fault directions F_i. A fault is identified by projecting the residual onto each of the residual subspaces and then determining which projections are nonzero.

Before the fault detection filter design (3.2) can begin, a system model with faults has to be found with the form (3.1). Twelve sensors and three actuators are associated with the linearized vehicle dynamics described in Section 2.3. The sensors measure the engine manifold airflow and engine speed, the vehicle forward, lateral and heave accelerations, the roll, pitch and yaw rate and the angular speed of each of the four wheels. The actuators control the engine throttle, the brake torque and the steering angle.

3.1 Sensor Fault Models

Sensor faults can be modeled as an additive term in the measurement equation

$$y = Cx + E_i\mu_i \tag{3.3}$$

where E_i is a column vector of zeros except for a one in the i^{th} position and where μ_i is an arbitrary time-varying real scalar. Since, for fault detection filter design, faults are expressed as additive terms to the system dynamics, a way must be found to convert the E_i sensor fault form of (3.3) to an equivalent F_i form as in (3.1). Let F_i satisfy

$$CF_i = E_i$$

and define a state estimation error e as

$$e = x - \hat{x} + F_i\mu_i$$

Using (3.2), the error dynamics are

$$\dot{e} = (A + LC)e + F_i\dot{\mu}_i - AF_i\mu_i \tag{3.4}$$

and a sensor fault E_i in (3.3) is equivalent to a two-dimensional fault F_i

$$\dot{x} = Ax + Bu + F_i m_i \qquad \text{with } F_i = \left[F_i^1, F_i^2\right]$$

where the directions F_i^1 and F_i^2 are given by

$$E_i = CF_i^1 \tag{3.5a}$$

$$F_i^2 = AF_i^1 \tag{3.5b}$$

An interpretation of the effect of a sensor fault on observer error dynamics follows from (3.4) where F_i^1 is the sensor fault rate $\dot{\mu}_i$ direction and F_i^2 is the sensor fault magnitude μ_i direction. This interpretation suggests a possible simplification when information about the spectral content of the sensor fault is available. If it is known that a sensor fault has persistent and significant high frequency components, such as in the case of a noisy sensor, the fault direction could be approximated by the F_i^1 direction alone. Or, if it is known that a sensor fault has only low frequency components, such as in the case of a bias, the fault direction could be approximated by the F_i^2 direction alone. For example, if a sensor were to develop a bias, a transient would be likely to appear in all fault directions but, in steady-state, only the residual associated with the faulty sensor should be nonzero.

Using the linearized dynamics of Section 2.3, an engine manifold airflow measurement is given by the first element of the system output (d.1). Therefore, any fault in the engine manifold airflow sensor can be modeled as an additive term in the measurement equation as in (3.3)

$$y = Cx + E_{y_{ma}}\mu_{y_{ma}}$$

where

$$E_{y_{m_a}} = \left[\begin{array}{cccccccccccc} 1, & 0, & 0, & 0, & 0, & 0, & 0, & 0, & 0, & 0, & 0, & 0 \end{array}\right]^T$$

and where $\mu_{y_{m_a}}$ is an arbitrary time-varying real scalar. An equivalent two-dimensional fault $F_{y_{m_a}}$ found by solving (3.5) is

$$F_{y_{m_a}} = \left[\begin{array}{cccccccccccccc} 1, & 0, & 0, & 0, & 0, & 0, & 0, & 0, & 0, & 0, & 0, & 0, & 0, & 0 \\ -22.42, & 306.69, & 0, & 0, & 0, & 0, & 0, & 0, & 0, & 0, & 0, & 0, & 0, & 0 \end{array}\right]^T$$

Other vehicle sensor fault directions are found in the same way.

3.2 Actuator Fault Models

A linear model partitioned to isolate first-order actuator dynamics can be expressed as

$$\left[\begin{array}{c} \dot{x} \\ \dot{x}_a \end{array}\right] = \left[\begin{array}{cc} A & B \\ 0 & -\omega \end{array}\right] \left[\begin{array}{c} x \\ x_a \end{array}\right] + \left[\begin{array}{c} 0 \\ \omega \end{array}\right] u$$

where x_a is a vector of actuator states. A fault in a control input is modeled as an additive term in the system dynamics. In the case of a fault appearing at the input of an actuator, that is the actuator command, the fault has the same direction as the associated column of the $[0,\ \omega]^T$ matrix. A fault appearing at the output of an actuator, the actuator position, has the same direction as the associated column of the $[B^T,\ 0]^T$ matrix. In the Berkeley nonlinear vehicle model, the actuator dynamics are relatively fast and, in an approximation made here, are removed from the system model. Thus, the control inputs are applied directly to the system through a column of the B matrix.

The engine throttle control is the first element of the system input so the direction of an engine throttle control fault is the first column of the B matrix from (d.1)

$$F_{u_a} = \left[\begin{array}{cccccccccccccc} 0, & 0, & 0, & 0, & 0, & 0, & 0, & 0, & 0, & 0, & 0, & 90.91, & 0, & 0 \end{array}\right]^T \qquad (3.6)$$

Fault directions for the brake torque and steering angle are developed in the same way and are given by

$$\begin{aligned} F_{u_{\tau_b}} &= \left[\begin{array}{cccccccccccccc} 0, & 0, & 0, & 0, & 0, & 0, & 0, & 0, & 0, & 0, & 0, & 0, & 1.25, & 0 \end{array}\right]^T \\ F_{u_\beta} &= \left[\begin{array}{cccccccccccccc} 0, & 0, & 0, & 0, & 0, & 0, & 0, & 0, & 0, & 0, & 0, & 0, & 0, & 80.0 \end{array}\right]^T \end{aligned}$$

CHAPTER 4
Fault Detection Filter Design

THE FAULT DETECTION FILTER DESIGN PROCESS consists of two steps. First, determine how many fault detection filters are needed and, if more than one, which filters will detect and identify which faults. In a detection filter, the state estimation error in response to a fault in the direction F_i remains in a state subspace $\mathcal{T}_i^*$, an unobservability subspace or detection space. See Appendix A for details. The ability to identify a fault, to distinguish one fault from another, requires for an observable system that the detection spaces be independent. Therefore, the number of faults that can be detected and identified by a fault detection filter is limited by the size of the state space and the sizes of the detection spaces associated with each of the faults. If the problem considered has more faults than can be accommodated by one fault detection filter, then a bank of filters will have to be constructed. The health monitoring system described in this section for a vehicle in a steady-state constant radius turn, considers fifteen system faults: twelve sensor faults and three actuator faults. Since the linearized vehicle models have either fourteen or twelve

states, clearly more than one fault detection filter is needed. As with the longitudinal mode system of (Douglas et al. 1995), a bank of four fault detection filters is built.

The second design step is to design the fault detection filters using eigenstructure assignment while making sure that the eigenvectors are not ill-conditioned. The essential feature of a fault detection filter is the detection space structure embedded in the filter dynamics. An eigenvector assignment design algorithm explicitly places eigenvectors to span these subspaces. An eigenvector assignment design algorithm also has to balance the objective of having well-conditioned eigenvectors for robustness against the objective of each fault being highly input observable for fault detection performance. System disturbances, sensor noise and system parameter variations are not considered in the fault detection filter designs described in this report. Note that they are considered in performance evaluation. For such a benign environment, the filter designs are based on spectral considerations only; there is little else that can be used to distinguish a good design from a bad design.

4.1 Fault Detection Filter Configuration

To determine how many and which faults may be included in a fault detection filter design, the detection spaces for each of the faults, also called unobservability subspaces, are formed. A detection space for a fault F_i is denoted by $\mathcal{T}_i^*$. First, the dimensions of the detection spaces are needed. Since the detection spaces are independent subspaces, the sum of their dimensions for any given fault detection filter cannot exceed the dimension of the state-space. Second, the detection spaces for any given fault detection filter are usually output separable and mutually detectable. These concepts are described in detail in Appendix A but briefly, output separability means that the output subspaces $C\mathcal{T}_i^*$ are independent. Mutual detectability means that the sum of the detection spaces $\sum \mathcal{T}_i^*$ is an unobservability subspace. This condition ensures that the spectrum of the detection filter can be assigned arbitrarily.

In practice it is just as easy to find a basis for the detection space as it is to find only the dimension. The method used here is suggested for numerical stability in (Wonham 1985)

and is described in Appendix A. Briefly, for a fault F_i, the approach is to find the minimal (C, A)-invariant subspace $\mathcal{W}_i^*$ that contains F_i and then to find the invariant zero directions of the triple (C, A, F_i), if any. With the invariant zero directions are denoted by $\mathcal{V}_i$, the minimal unobservability subspace $\mathcal{T}_i^*$ is given by

$$\mathcal{T}_i^* = \mathcal{W}_i^* + \mathcal{V}_i$$

The linear model of Section 2.3 has either fourteen or twelve states, twelve sensors and three controls. As explained in Section 3, each sensor and each actuator is to be monitored for a fault. It turns out that for all twelve sensor faults and for the steering actuator fault described in Section 3, the detection spaces are given by the fault directions themselves, that is,

$$\mathcal{T}_i^* = \text{Im}\, F_i$$

For the throttle actuator fault, $CF_{u_\alpha} = 0$, so the detection space for this fault is

$$\mathcal{T}_{u_\alpha}^* = \text{Im}\,[F_{u_\alpha}, AF_{u_\alpha}]$$

For the brake actuator fault, $CF_{u_{\tau_b}} \neq 0$ in the reduced-order model used for filter design. However, $CF_{u_{\tau_b}} = 0$ in the full-order model so $F_{u_{\tau_b}}$ is considered to be a very weakly observable direction. The detection space for brake actuator fault is taken to be second-order as for the throttle fault

$$\mathcal{T}_{u_{\tau_b}}^* = \text{Im}\left[F_{u_{\tau_b}}, AF_{u_{\tau_b}}\right]$$

Before designing any fault detection filters, it is useful to determine which faults are output separable. A detection filter designed with faults that are not output separable will generate co-linear residuals and the faults cannot be isolated. Such faults are also considered detection equivalent (Beard 1971). Output separability of two faults F_i and F_j is determined by checking for column independence of realizations for $C\mathcal{T}_i$ and $C\mathcal{T}_j$. Performing this check reveals that the throttle actuator and air mass sensor faults are not

output separable because

$$CT^*_{u_\alpha} = \begin{bmatrix} 1 \\ 0 \\ 0 \\ 0 \\ 0 \\ 0 \\ 0 \\ 0 \\ 0 \\ 0 \\ 0 \\ 0 \end{bmatrix} \qquad CT^*_{y_{m_a}} = \begin{bmatrix} 1 & 0 \\ 0 & 0.9968 \\ 0 & 0.0597 \\ 0 & -0.0001 \\ 0 & -0.0016 \\ 0 & 0 \\ 0 & 0 \\ 0 & 0 \\ 0 & 0 \\ 0 & 0 \\ 0 & 0.0404 \\ 0 & 0.0340 \end{bmatrix}$$

Since $CF_{y_{m_a}} = CAF_{u_\alpha}$, the throttle actuator and air mass sensor faults would not normally be part of a single fault detection filter design. However, it is possible to include both in one filter if the sensor fault is approximated as a one-dimensional fault. As explained in Section 3.1, the direction of the sensor fault magnitude is $AF_{y_{m_a}}$ while the direction of the fault rate is $F_{y_{m_a}}$. The throttle actuator and air mass sensor faults become output separable if only the sensor fault magnitude direction is used. This design decision could allow a noisy but zero mean sensor fault to remain undetected. However, a throttle actuator fault could never stimulate the air mass sensor fault residual. Also, since the throttle fault detection space is spanned by F_{u_α} and AF_{u_α}, an air mass sensor fault rate will stimulate the throttle fault residual. Finally, as long as an air mass sensor fault spectral components are low frequency, the two faults should be detectable and isolated.

Another consideration in grouping the faults among the fault detection filters is to group faults which are robust to system nonlinearities. Note that an actuator fault changes the vehicle operating point possibly introducing nonlinear effects into all measurements. The nonlinear effect is small if the residual response is small compared to that for some nominal fault. Also, sensor faults that are open-loop are easily isolated since they do not stimulate any dynamics. One approach to fault grouping is to always group actuator and sensor faults with different fault detection filters.

Finally, usually an attempt is made to group as many faults as possible in each filter.

When full-order filters are used, this approach minimizes the number of filters needed. When reduced-order filters are used, this approach minimizes the order of each complementary space and, therefore, the order of each reduced-order filter. Note that each fault included in a fault detection filter design imposes more constraints on the filter eigenvectors. Sometimes, the objective of obtaining well-conditioned filter eigenvectors imposes a tradeoff between robustness and the reduced-order filter size.

Given the above considerations, fault detection filters are designed for the following groups of faults:

Fault detection filter 1.

$F_{y_{\omega_e}}$: Engine speed sensor.

$F_{y_{\ddot{y}}}$: Lateral acceleration sensor.

$F_{y_{\ddot{z}}}$: Vertical acceleration sensor.

$F_{y_{\dot{\theta}}}$: Pitch rate sensor.

Fault detection filter 2.

$F_{y_{\ddot{x}}}$: Longitudinal acceleration sensor.

$F_{y_{\dot{\phi}}}$: Roll rate sensor.

$F_{y_{\dot{\epsilon}}}$: Yaw rate sensor.

$F_{y_{\omega_e}}$: Engine speed sensor.

Fault detection filter 3.

$F_{y_{\omega_{fl}}}$: Front left wheel speed sensor.

$F_{y_{\omega_{fr}}}$: Front right wheel speed sensor.

$F_{y_{\omega_{rl}}}$: Rear left wheel speed sensor.

$F_{y_{\omega_{rr}}}$: Rear right wheel speed sensor.

Fault detection filter 4.

F_{u_α} : Throttle angle actuator.

$F_{u_{\tau_b}}$: Brake torque actuator.

F_{u_β} : Steering angle actuator.

$F_{y_{m_a}}$: Manifold air mass sensor.

Showing that the fault sets are mutually detectable involves calculating invariant zeros of each triple $(C, A, F_1), \ldots, (C, A, F_q)$ and then showing that these are the same invariant zeros as of the triple $(C, A, [F_1, \ldots, F_q])$. For example, for the first fault detection filter, define the sets of invariant zeros

$$\begin{aligned}
\Omega_{y_{\omega_e}} &= \Omega(C, A, F_{y_{\omega_e}}) \\
\Omega_{y_{\ddot{y}}} &= \Omega(C, A, F_{y_{\ddot{y}}}) \\
\Omega_{y_{\ddot{z}}} &= \Omega(C, A, F_{y_{\ddot{z}}}) \\
\Omega_{y_{\dot{\theta}}} &= \Omega(C, A, F_{y_{\dot{\theta}}}) \\
\Omega_y &= \Omega(C, A, [F_{y_{\omega_e}}, F_{y_{\ddot{y}}}, F_{y_{\ddot{z}}}, F_{y_{\dot{\theta}}}])
\end{aligned}$$

where $\Omega(C, A, F_i)$ means the set of invariant zeros of the triple (C, A, F_i). The first fault detection filter is mutually detectable because

$$\Omega_y = \Omega_{y_{\omega_e}} + \Omega_{y_{\ddot{y}}} + \Omega_{y_{\ddot{z}}} + \Omega_{y_{\dot{\theta}}}$$

4.2 Eigenstructure Placement

The fault detection filters are found using a left eigenvector assignment algorithm described in Appendix B. Since the calculations are somewhat long and they are the same for each detection filter, the calculation details are given for only the actuator fault detection filter and one of the sensor fault detection filters. Algorithm B.1 is applied to the design of fault detection filters for the third fault group, which has the four wheel speed sensors, and the fourth fault group, which has the throttle actuator, the brake actuator, the steering actuator and the manifold air mass sensor.

4.2.1 Sensor Fault Design

This section presents the details of a fault detection filter design for fault group three, the four wheel speed sensors. The twelve state reduced-order linear model derived in Section 2.3 is used. The first step is to find the dimension of each detection space. This was discussed in Section 4.1 where it was shown that the detection spaces are given by the fault directions themselves, that is, $\mathcal{T}_i^* = \operatorname{Im} F_i$. The fault directions assigned to the third fault detection filter are all sensor faults and all have dimension two

$$\begin{aligned}
\nu_{y_{w_{fl}}} &= \dim \mathcal{T}^*_{y_{w_{fl}}} = 2 \\
\nu_{y_{w_{fr}}} &= \dim \mathcal{T}^*_{y_{w_{fr}}} = 2 \\
\nu_{y_{w_{rl}}} &= \dim \mathcal{T}^*_{y_{w_{rl}}} = 2 \\
\nu_{y_{w_{rr}}} &= \dim \mathcal{T}^*_{y_{w_{rr}}} = 2
\end{aligned}$$

The dimension of the fault detection filter complementary space $\mathcal{T}_0$ is also needed. The complementary space is any subspace independent of the detection spaces that completes the state-space. Thus, for the first fault detection filter

$$\mathcal{X} = \mathcal{T}^*_{y_{w_{fl}}} \oplus \mathcal{T}^*_{y_{w_{fr}}} \oplus \mathcal{T}^*_{y_{w_{rl}}} \oplus \mathcal{T}^*_{y_{w_{rr}}} \oplus \mathcal{T}_0$$

and the dimension of $\mathcal{T}_0$ is four

$$\begin{aligned}
\nu_0 &= n - \nu_{y_{w_{fl}}} - \nu_{y_{w_{fr}}} - \nu_{y_{w_{rl}}} - \nu_{y_{w_{rr}}} \\
&= 12 - 2 - 2 - 2 - 2 \\
&= 4
\end{aligned}$$

Next define the complementary fault sets. There are four faults $F_{y_{w_{fl}}}$, $F_{y_{w_{fr}}}$, $F_{y_{w_{rl}}}$ and $F_{y_{w_{rr}}}$ so there are five complementary fault sets which are:

$$\hat{F}_{y_{w_{fl}}} = \left[F_{y_{w_{fr}}}, F_{y_{w_{rl}}}, F_{y_{w_{rr}}}\right] \tag{4.1a}$$

$$\hat{F}_{y_{w_{fr}}} = \left[F_{y_{w_{fl}}}, F_{y_{w_{rl}}}, F_{y_{w_{rr}}}\right] \tag{4.1b}$$

$$\hat{F}_{y_{w_{rl}}} = \left[F_{y_{w_{fl}}}, F_{y_{w_{fr}}}, F_{y_{w_{rr}}}\right] \tag{4.1c}$$

$$\hat{F}_{y_{w_{rr}}} = \left[F_{y_{w_{fl}}}, F_{y_{w_{fr}}}, F_{y_{w_{rl}}}\right] \tag{4.1d}$$

$$\hat{F}_0 = \left[F_{y_{w_{fl}}}, F_{y_{w_{fr}}}, F_{y_{w_{rl}}}, F_{y_{w_{rr}}}\right] \tag{4.1e}$$

Now choose the fault detection filter closed-loop eigenvalues. Since the system model includes no sensor noise, no disturbances and no parameter variations, there is little basis for preferring one set of detection filter closed-loop eigenvalues over another. The poles are chosen here to give a reasonable response time but are not unrealistically fast. The assigned eigenvalues are

$$\begin{aligned}
\Lambda_{y_{w_{fl}}} &= \{-3, -10\} \\
\Lambda_{y_{w_{fr}}} &= \{-4, -9\} \\
\Lambda_{y_{w_{rl}}} &= \{-5, -8\} \\
\Lambda_{y_{w_{rr}}} &= \{-6, -7\} \\
\Lambda_0 &= \{-11, -12, -13, -14\}
\end{aligned}$$

The next step is to find the closed-loop fault detection filter left eigenvectors. For each eigenvalue $\lambda_{i_j} \in \Lambda_i$, the left eigenvectors v_{i_j} generally are not unique and must be chosen from a subspace as $v_{i_j} \in V_{i_j}$ where V_{i_j} and another space W_{i_j} are found by solving

$$\begin{bmatrix} A^T - \lambda_{i_j} I & C^T \\ \hat{F}_i^T & 0 \end{bmatrix} \begin{bmatrix} V_{i_j} \\ W_{i_j} \end{bmatrix} = \begin{bmatrix} 0 \\ 0 \end{bmatrix} \tag{4.2}$$

There are twelve V_{i_j} associated with twelve eigenvalues. Only two V_{i_j}, the two associated with the front left wheel speed sensor fault, are shown here because this intermediate result is easily reproduced. They are shown in Appendix E. As explained in Appendix B and (Douglas and Speyer 1995b), to help desensitize the fault detection filter to parameter variations, the left eigenvectors are chosen from $v_{i_j} \in V_{i_j}$ as the set with the greatest degree of linear independence. The degree of linear independence is indicated by the smallest singular value of the matrix formed by the left eigenvectors. Upper bounds on the singular values of the left eigenvectors are given by the singular values of

$$V = [V_{0_1}, V_{0_2}, V_{0_3}, V_{0_4}, V_{y_{w_{fl1}}}, V_{y_{w_{fl2}}}, V_{y_{w_{fr1}}}, V_{y_{w_{fr2}}}, V_{y_{w_{rl1}}}, V_{y_{w_{rl2}}}, V_{y_{w_{rr1}}}, V_{y_{w_{rr2}}}]$$

These singular values are

$$\sigma(V) = \{3.4641,\ 3.4641,\ 3.4641,\ 3.4641,\ 2.5763,\ 2.0626,$$
$$1.9404,\ 1.1563,\ 0.0627,\ 0.0431,\ 0.0099,\ 0.0014\} \quad (4.3)$$

If the left eigenvector singular value upper bounds were small, then all possible combinations of detection filter left eigenvectors would be ill-conditioned and the filter eigenstructure would be sensitive to small parameter variations. Since (4.3) indicates that the upper bounds are not small, continue by looking for a set of fault detection filter left eigenvectors that are reasonably well-conditioned. For this case, one possible set of left eigenvectors from the set V nearly meets the upper bound, is well-conditioned and is given in Appendix E. The singular values of this set of detection filter left eigenvectors are

$$\sigma(\tilde{V}) = \{1.82,\ 1.46,\ 1.37,\ 1.00,\ 1.00,\ 1.00, 1.00,\ 0.818,\ 0.0443,\ 0.0305,\ 0.0070,\ 0.0010\}$$

Since the difference between the largest and the smallest singular values is only three orders of magnitude, the detection filter gain will be reasonably small and the filter eigenstructure should not be sensitive to small parameter variations.

The fault detection filter gain L is found by solving

$$\tilde{V}^T L = \tilde{W}^T \quad (4.4)$$

where $\tilde{V}$ is the matrix of left eigenvectors as found above, and $\tilde{W}$ is a matrix of vectors w_{i_j} which satisfy (b.10)

$$\begin{bmatrix} A^T - \lambda_{i_j} I & C^T \\ \hat{F}_i^T & 0 \end{bmatrix} \begin{bmatrix} v_{i_j} \\ w_{i_j} \end{bmatrix} = \begin{bmatrix} 0 \\ 0 \end{bmatrix}$$

If the left eigenvector v_{i_j} is a linear combination of the columns of V_{i_j}, w_{i_j} is the same linear combination of the columns of W_{i_j} where V_{i_j} and W_{i_j} are from (4.2). The $\tilde{W}$ matrix is given in Appendix E. The detection filter gain is found from (4.4) and is also given in Appendix E.

To complete the detection filter design, output projection matrices $\hat{H}_{y_{w_{fl}}}$, $\hat{H}_{y_{w_{fr}}}$, $\hat{H}_{y_{w_{rl}}}$ and $\hat{H}_{y_{w_{rr}}}$ are needed to project the residual along the respective output subspaces $C\hat{T}^*_{y_{w_{fl}}}$, $C\hat{T}^*_{y_{w_{fr}}}$, $C\hat{T}^*_{y_{w_{rl}}}$ and $C\hat{T}^*_{y_{w_{rr}}}$. What this means is that, for example, $\hat{T}^*_{y_{w_{fl}}}$ becomes the unobservable subspace of the pair $(\hat{H}_{y_{w_{fl}}} C, A + LC)$. Remember that by the definition of

the complementary faults (4.1), faults $F_{y_{w_{fr}}}$, $F_{y_{w_{rl}}}$ and $F_{y_{w_{rr}}}$ lie in $\hat{T}^*_{y_{w_{fl}}}$ and fault $F_{y_{w_{fl}}}$ does not. The effect is that the projected residual is driven by fault $F_{y_{w_{fl}}}$ and only fault $F_{y_{w_{fl}}}$ as shown in Figure 4.3.

A projection $\hat{H}_i$ is computed by first finding a basis for the range space of $C\hat{T}^*_i$ where again, $\hat{T}^*_i$ is any basis for the detection space $\hat{T}^*_i$. This is done by finding the left singular vectors of $C\hat{T}^*_i$. Denote this basis for now as h_i. Then $\hat{H}_i$ is given by

$$\hat{H}_i = I - h_i h_i^T$$

An output projection for the front left wheel speed sensor is given in (e.2) of Appendix E.

In summary, a fault detection filter for the system with sensor faults $E_{y_{w_{fl}}}$, $E_{y_{w_{fr}}}$, $E_{y_{w_{rl}}}$ and $E_{y_{w_{rr}}}$ as in (3.3)

$$\begin{aligned} \dot{x} &= Ax + Bu \\ y &= Cx + Du + E_{y_{w_{fl}}}\mu_{y_{w_{fl}}} + E_{y_{w_{fr}}}\mu_{y_{w_{fr}}} + E_{y_{w_{rl}}}\mu_{y_{w_{rl}}} + E_{y_{w_{rr}}}\mu_{y_{w_{rr}}} \end{aligned}$$

is equivalent to a fault detection filter for the system with faults $F_{y_{w_{fl}}}$, $F_{y_{w_{fr}}}$, $F_{y_{w_{rl}}}$ and $F_{y_{w_{rr}}}$ as in (3.5)

$$\begin{aligned} \dot{x} &= Ax + Bu + F_{y_{fl}} m_{y_{w_{fl}}} + F_{y_{w_{fr}}} m_{y_{w_{fr}}} + F_{y_{w_{rl}}} m_{y_{w_{rl}}} + F_{y_{w_{rr}}} m_{y_{w_{rr}}} \\ y &= Cx + Du \end{aligned}$$

and has the form

$$\begin{aligned} \dot{\hat{x}} &= (A + LC)\hat{x} + (B + LD)u - Ly \\ z_{y_{w_{fl}}} &= \hat{H}_{y_{w_{fl}}}(C\hat{x} + Du - y) \\ z_{y_{w_{fr}}} &= \hat{H}_{y_{w_{fr}}}(C\hat{x} + Du - y) \\ z_{y_{w_{rl}}} &= \hat{H}_{y_{w_{rl}}}(C\hat{x} + Du - y) \\ z_{y_{w_{rr}}} &= \hat{H}_{y_{w_{rr}}}(C\hat{x} + Du - y) \end{aligned}$$

with L and the $\hat{H}_{y_{w_{fl}}}$, $\hat{H}_{y_{w_{fr}}}$, $\hat{H}_{y_{w_{rl}}}$ and $\hat{H}_{y_{w_{rr}}}$ given by (e.1) and (e.2). Calculations for the detection filters for the other two sensor fault groups 1 and 2 are carried out in the same way and are not shown here.

Figures 4.1, 4.2 and 4.3 show the singular value frequency responses of fault detection filters for fault groups one, two and three, the sensor fault groups. The frequency responses are from all faults for which the filter has been designed to each of the filter residuals. The singular values show that each residual only responds to the fault it was designed to detect when no noise or parametric uncertainties are present.

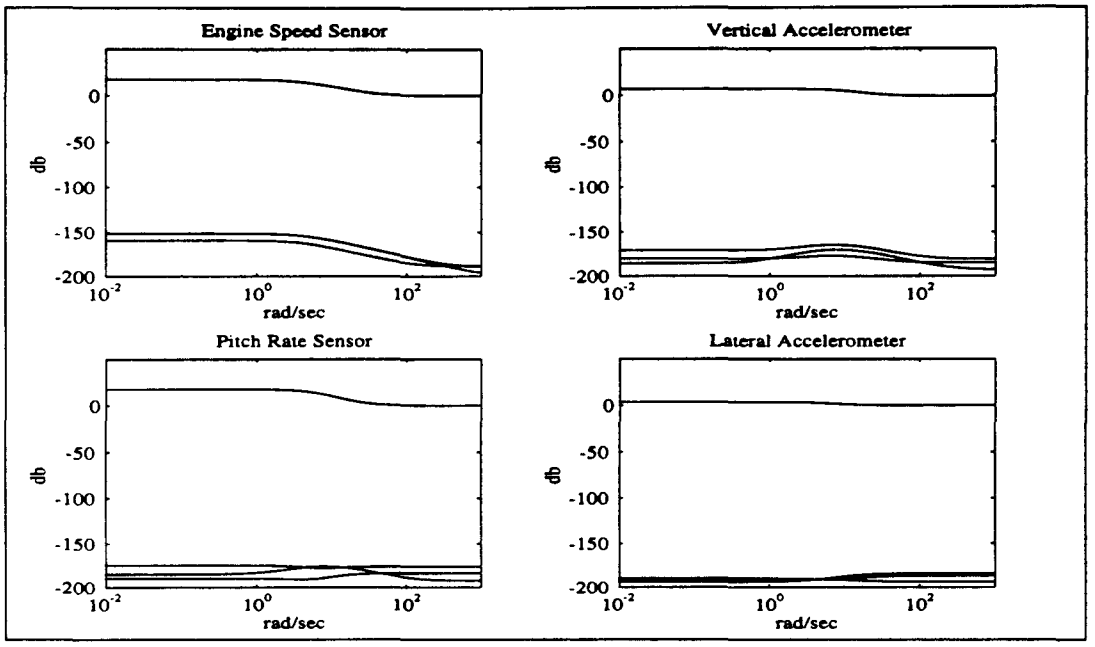

Figure 4.1: Singular value frequency response from all faults to residuals of fault detection filter one.

4.2.2 Actuator Fault Design

This section presents the details of a fault detection filter design for fault group four. The fault directions assigned to fault group four are the throttle actuator, the brake actuator, the steering actuator and the manifold air mass sensor faults. The fourteen state reduced-order linear model derived in Section 2.3 is used.

The design procedure is similar to the previous section but does have a twist. As discussed in Section 4.1, a reduced-order air mass sensor fault is used to achieve output separability with the throttle actuator fault. The dimension of each detection space was

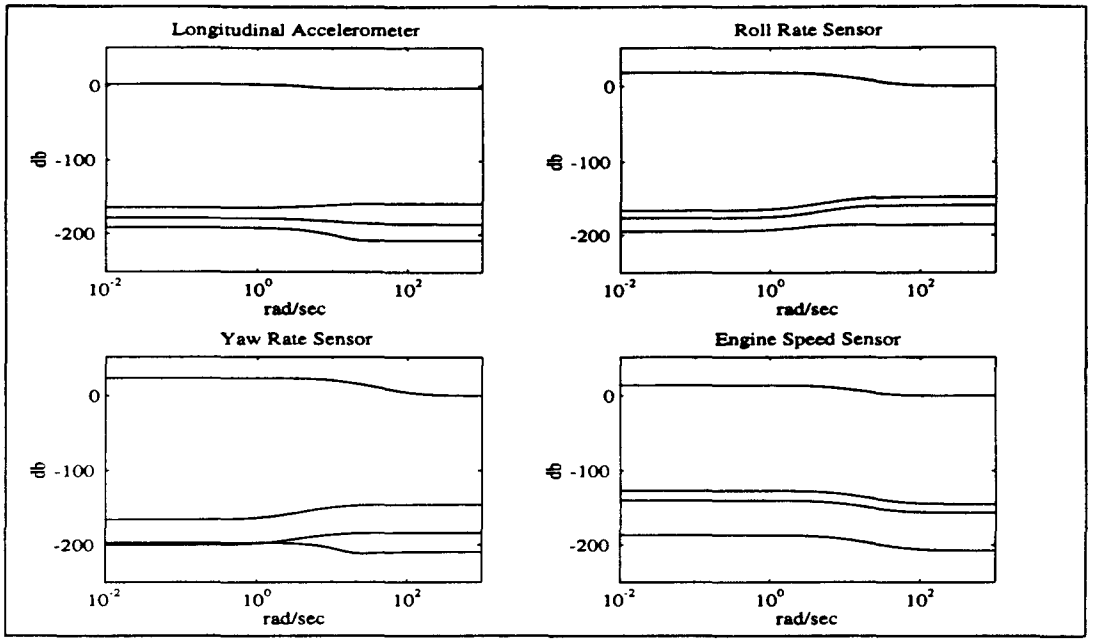

Figure 4.2: Singular value frequency response from all faults to residuals of fault detection filter two.

found in Section 4.1 as

$$\begin{aligned} \nu_{u_\alpha} &= \dim \mathcal{T}^*_{u_\alpha} = 2 \\ \nu_{u_{\tau_b}} &= \dim \mathcal{T}^*_{u_{\tau_b}} = 2 \\ \nu_{u_{beta}} &= \dim \mathcal{T}^*_{u_\beta} = 1 \\ \nu_{y_{m_a}} &= \dim \mathcal{T}^*_{y_{m_a}} = 1 \end{aligned}$$

and the dimension of the fault detection filter complementary space $\mathcal{T}_0$ where

$$\mathcal{X} = \mathcal{T}^*_{u_\alpha} \oplus \mathcal{T}^*_{u_{\tau_b}} \oplus \mathcal{T}^*_{u_\beta} \oplus \mathcal{T}^*_{y_{m_a}} \oplus \mathcal{T}_0$$

is eight

$$\begin{aligned} \nu_0 &= n - \nu_{u_\alpha} - \nu_{u_{\tau_b}} - \nu_{u_\beta} - \nu_{y_{m_a}} \\ &= 14 - 2 - 2 - 1 - 1 \\ &= 8 \end{aligned}$$

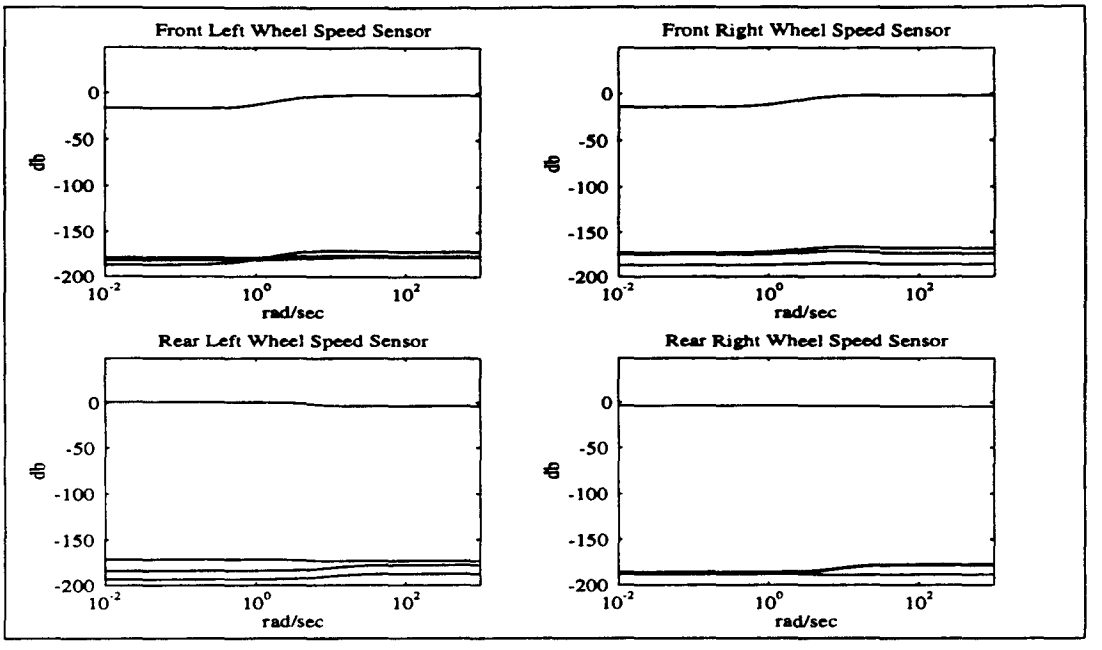

Figure 4.3: Singular value frequency response from all faults to residuals of fault detection filter three.

Next define the complementary faults sets. There are four faults F_{u_α}, $F_{u_{\tau_b}}$, F_{u_β} and $F_{y_{m_a}}$ so there are five complementary fault sets which are:

$$\hat{F}_{u_\alpha} = \left[F_{u_{\tau_b}}, F_{u_\beta}, F_{y_{m_a}}\right] \tag{4.5a}$$

$$\hat{F}_{u_{\tau_b}} = \left[F_{u_\alpha}, F_{u_\beta}, F_{y_{m_a}}\right] \tag{4.5b}$$

$$\hat{F}_{u_\beta} = \left[F_{u_\alpha}, F_{u_{\tau_b}}, F_{y_{m_a}}\right] \tag{4.5c}$$

$$\hat{F}_{y_{m_a}} = \left[F_{u_\alpha}, F_{u_{\tau_b}}, F_{u_\beta}\right] \tag{4.5d}$$

$$\hat{F}_0 = \left[F_{u_\alpha}, F_{u_{\tau_b}}, F_{u_\beta}, F_{y_{m_a}}\right] \tag{4.5e}$$

Now choose the fault detection filter closed-loop eigenvalues.

$$\Lambda_{u_\alpha} = \{-4, -9\}$$

$$\Lambda_{u_{\tau_b}} = \{-5, -8\}$$

$$\Lambda_{u_\beta} = \{-6\}$$

$$\Lambda_{y_{m_a}} = \{-7\}$$

$$\Lambda_0 = \{-10, -11, -12, -13, -14, -15, -16, -17\}$$

The next step is to find the closed-loop fault detection filter left eigenvectors. As in Section 4.2.1, the left eigenvectors v_{i_j} for each eigenvalue $\lambda_{i_j} \in \Lambda_i$ generally are not unique and must be chosen from a subspace as $v_{i_j} \in V_{i_j}$ where V_{i_j} is found by solving

$$\begin{bmatrix} A^T - \lambda_{i_j} I & C^T \\ \hat{F}_i^T & 0 \end{bmatrix} \begin{bmatrix} V_{i_j} \\ W_{i_j} \end{bmatrix} = \begin{bmatrix} 0 \\ 0 \end{bmatrix} \tag{4.6}$$

There are fourteen V_{i_j} associated with fourteen eigenvalues. Upper bounds on the singular values of the left eigenvectors are given by the singular values of

$$V = [V_{u_{\tau_{b1}}}, V_{u_{\tau_{b2}}}, V_{0_1}, V_{0_2}, V_{0_3}, V_{0_4}, V_{0_5}, V_{0_6}, V_{0_7}, V_{0_8}, V_{u_{\alpha_1}}, V_{u_{\alpha_2}}, V_{u_\beta}, V_{y_{m_\alpha}}] \tag{4.7}$$

These singular values are

$$\begin{aligned} \sigma(V) = \{&3.74,\ 3.74,\ 3.74,\ 3.74,\ 3.74,\ 3.74,\ 3.71, \\ &2.19,\ 1.65,\ 0.734,\ 0.466,\ 0.0918,\ 0.0272,\ 0.0005\} \end{aligned} \tag{4.8}$$

Since (4.8) indicates that the upper bounds are not small, continue by looking for a set of fault detection filter left eigenvectors that are reasonably well-conditioned. One possible choice is, given in Appendix E, has the following singular values

$$\begin{aligned} \sigma(\tilde{V}) = \{&1.73,\ 1.47,\ 1.39,\ 1.34,\ 1.02,\ 1.00,\ 1.00, \\ &1.00,\ 0.955,\ 0.350,\ 0.117,\ 0.0073,\ 0.0026,\ 0.0005\} \end{aligned}$$

Since these singular values are quite close to their respective upper bounds, the detection filter gain should not be large and the filter eigenstructure should not be sensitive to small parameter variations. As in Section 4.2.1, the fault detection filter gain L is found by solving

$$\tilde{V}^T L = \tilde{W}^T \tag{4.9}$$

where the columns of $\tilde{V}$ and $\tilde{W}$ are found from (4.6). Both $\tilde{W}$ and L are given in Appendix E. Output projection matrices $\hat{H}_{u_\alpha}$, $\hat{H}_{u_{\tau_b}}$, $\hat{H}_{u_\beta}$ and $\hat{H}_{y_{m_\alpha}}$ are needed to complete the fault

detection filter design These are found in the same way as for the sensor fault example of Section 4.2.1 and are given in Appendix E.

A note should be made regarding the throttle actuator fault residual. By the definition of the complementary faults (4.5), $F_{u_{\tau_b}}$, F_{u_β} and $F_{y_{m_a}}$ lie in $\hat{T}^*_{u_\alpha}$ while F_{u_α} does not. The effect is that the projected residual is not driven by fault $F_{u_{\tau_b}}$, F_{u_β} or $F_{y_{m_a}}$. Now recall that $F_{y_{m_a}}$ is a reduced-order approximation for $E_{y_{m_a}}$ so the throttle actuator residual is not only driven by F_{u_α}, but also the part of $E_{y_{m_a}}$ not modeled by $F_{y_{m_a}}$. As shown in Figure 4.4, the throttle actuator residual can only isolate faults well at low frequency while other residuals isolate all faults.

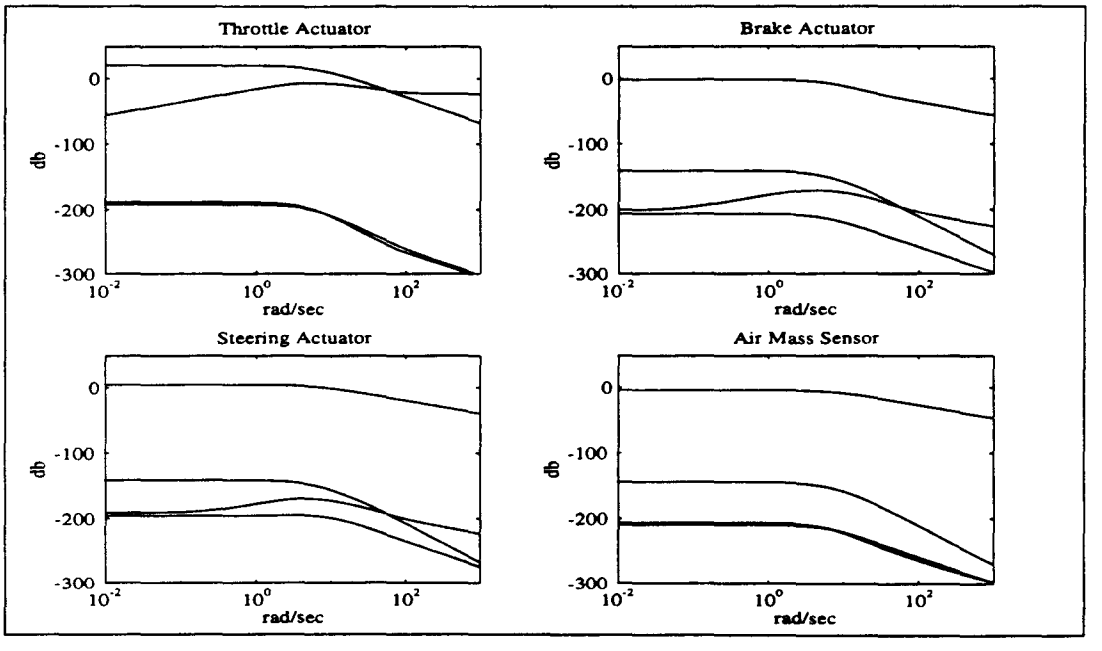

Figure 4.4: Singular value frequency response from all faults to residuals of fault detection filter four.

CHAPTER 5
Fault Detection Filter Evaluation

FAULT DETECTION FILTER PERFORMANCE is evaluated using the nonlinear simulation discussed in Section 2.1. The fault detection filters designed in Sections 4.2.1 and 4.2.2 are tested on smooth and rough roads. Performance is evaluated with respect to robustness to model nonlinearities and road noise. The performance of a longitudinal mode fault detection filter described in (Douglas et al. 1995) is also evaluated.

5.1 Fault Detection Filter Evaluation On A Curved Road

Fault detection filter performance is evaluated using the nonlinear vehicle simulation of Section 2.1. Sensor fault detection performance is evaluated by introducing a sensor bias into the data provided by the nonlinear simulation. In the most benign test, the nonlinear vehicle simulation is run in a steady state turn with $24.87\frac{m}{sec}$ forward speed while a bias is added to one of the sensor outputs. The turn is acheived using a 0.005 rad. steering angle. In this test, the operating point is the same as that used to derive the linearized dynamics

for the fault detection filter design. Furthermore, the vehicle dynamics are not stimulated resulting in data that is essentially linear. Thus, the fault detection filter is operating in a nominal environment and the test does not provide much useful information. The results of these tests are not shown here.

In a more useful test, the filters operate at an off-nominal condition, that is, the vehicle operates in a steady state condition but not the same one used to generate the linearized dynamics. These tests are discussed in Section 5.1.1. Dynamic disturbances are introduced by simulating a rough road surface as in Section 2.1.2. Fault detection filter testing in the presence of dynamic disturbances is discussed in Section 5.1.2.

5.1.1 Evaluation On Smooth Road

In this section, the fault detection filters of Section 4.2 are tested at an off-nominal operating point, that is, the vehicle operates in a steady state condition but not the same one used to generate the linearized dynamics. This is achieved by increasing the throttle two degrees from the nominal value causing the steady state vehicle speed to be about two meters per second faster than the nominal. The road is flat and smooth so only vehicle nonlinearities corrupt the filter residuals. If the vehicle dynamics were linear, the increased throttle setting would have only a transient effect, if any, on the linear fault detection filter state estimates. The state estimate errors and the filter residuals would asymptotically go to zero. Since the vehicle dynamics are not linear and the vehicle operating condition is not the same as it would be if the dynamics were linear, the filter state estimates and the residuals are not zero.

Since most residuals are not zero, as is to be expected, the natural question to ask is what magnitude residual should be considered small. The answer lies in comparing the size of a nonzero residual due to non-linearities and the size of a nonzero residual due to a fault. A residual scaling factor is chosen such that when a fault is introduced into the *linearized* dynamics the magnitude of the corresponding reduced-order fault detection filter residual is one. Since all residuals generated by the off-nominal operating condition have magnitude less than 0.25, they should not be easily mistaken for residuals generated by a fault.

Of course, the size of the residual is proportional to the size of the fault. The size of the fault used for finding the residual scaling factors is determined as follows. For most sensors, the size of the fault is given by the difference in magnitude between the sensor output at the nominal and off-nominal steady state operating conditions. For some sensors, such as the accelerometers and the angular rate sensors, the output is zero in any steady state condition and another method has to be used. For the longitudinal accelerometer, the size of the fault is given as the largest transient value of the sensor output while a two-degree step throttle command takes the vehicle from the nominal to off-nominal condition. For the lateral and vertical accelerometers, even the transient is small during an acceleration maneuver. Thus the same nominal fault value used for longitudinal acceleration fault is also used for the lateral and heave accelerometers. The pitch, roll and yaw rate sensors are treated the same way as the lateral and heave accelerometers. The value $0.02\frac{\text{rad}}{\text{sec}}$ is chosen as a value for vehicle rotation rates reasonably encountered during normal vehicle operation.

Figure 5.1 shows the magnitudes of the residuals for the four fault detection filters derived from the first fault design group: the engine speed sensor, lateral and vertical accelerometers and pitch rate sensor. A sensor bias fault is added after two seconds when filter initialization errors have died out. Only one sensor fault is added at a time; simultaneous faults are not allowed. It is important to note that when any of the sensor faults from the first fault design group occur, the residuals associated with a fault detection filter designed for other faults have no meaning. This is why only four residuals are shown in each plot of Figures 5.1, 5.2, 5.3, 5.4 and 5.5 while sixteen residuals are generated by the entire fault detection system. Distinguishing a meaningful residual from a non-meaningful residual is left to the residual processing system described in sections 6 and 7. The residual associated with the fault quickly approaches one and other residuals *in the fault group* remain unaffected.

Figures 5.2 and 5.3 show the residuals for the four fault detection filters derived from the second and third sensor fault design groups. Residual scaling factors are chosen in the same way as for the first fault design group. The fault detection filter performance indicated by

Figures 5.2 and 5.3 is the same as that indicated by Figure 5.1.

The performance of the filter for the fourth fault group which includes actuator faults is shown in Figure 5.4. A throttle fault is simulated by sending a two-degree step throttle command to the nonlinear simulation but not to the fault detection filter. Even though a throttle fault stimulates the vehicle nonlinear dynamics and the residual associated with other faults, Figure 5.4 shows that both positive and negative throttle faults are clearly identifiable from other faults. A brake fault is simulated by applying a brake torque just large enough to slow the vehicle from $25\frac{m}{sec}$ to $21\frac{m}{sec}$. This changes the vehicle steady state operating point by the same amount as a minus four degree throttle fault. Figure 5.4 shows that the brake fault is clearly identified. A steering fault is simulated by a 0.001 rad. steering angle bias. Recall that the nominal turn is acheived with a 0.005 rad. steering angle. Figure 5.4 shows that the steering fault is clearly identified.

An interesting observation of the throttle actuator residual behavior follows from the dicussion of Section 4.1 and is illustrated in Figure 5.5. Since one direction of the throttle actuator fault corresponds to the air mass sensor fault rate, a bias fault in the air mass sensor causes a response in the throttle actuator residual. Since the throttle actuator residual only responds to air mass sensor fault rate, the residual response is transient and dies out quickly. There should be no problem distinguishing throttle actuator and air mass sensor faults as long as the air mass sensor fault only has low frequency components.

5.1.2 Evaluation On Rough Road

Tests performed on the fault detection filters in this section closely follow those of the last section except that the road is no longer smooth. The same types and sizes of faults are used here as in Section 5.1.1

It has already been demonstrated that when no road noise is present, filter residuals not associated with a given sensor fault do not respond when that fault occurs. Therefore, only residuals associated with a fault are shown in the plots. For comparison, the residuals for the no fault case are also given.

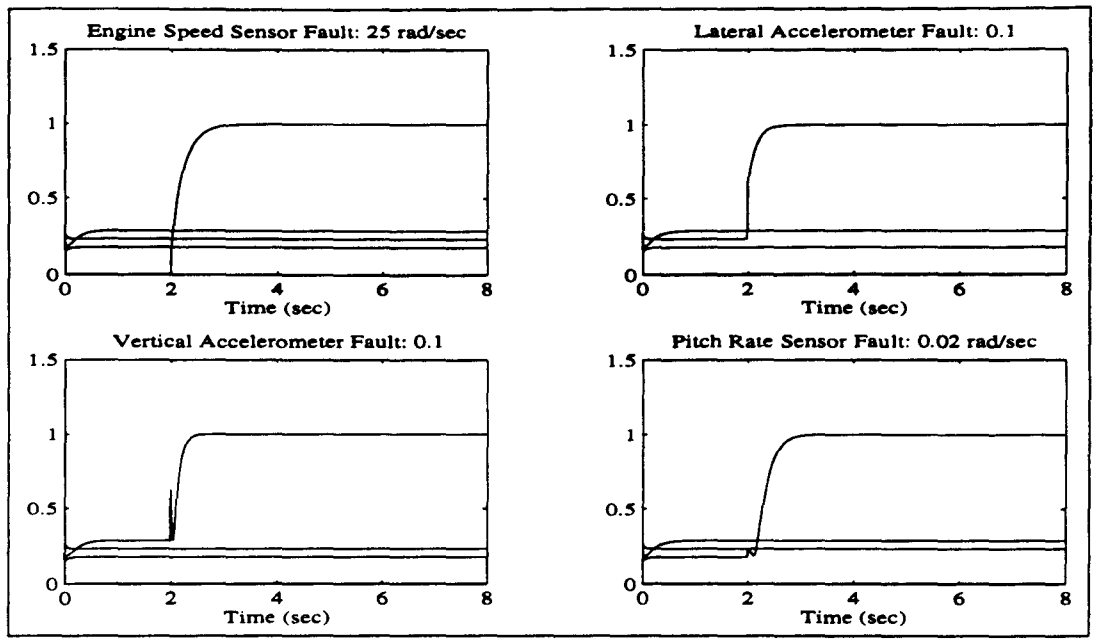

Figure 5.1: Residuals for fault detection filter one.

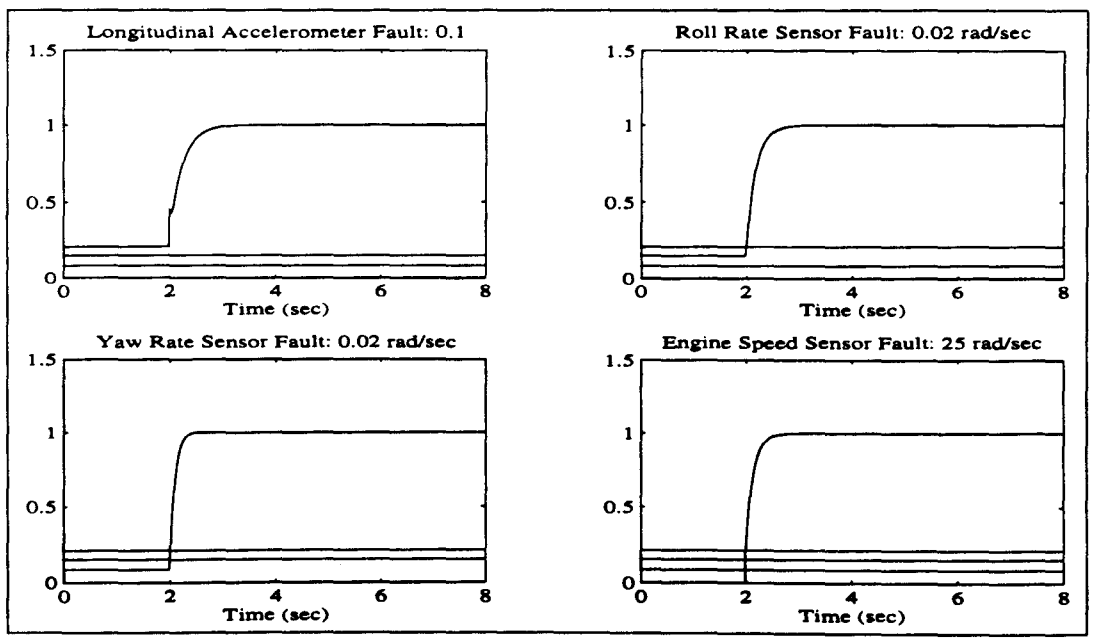

Figure 5.2: Residuals for fault detection filter two.

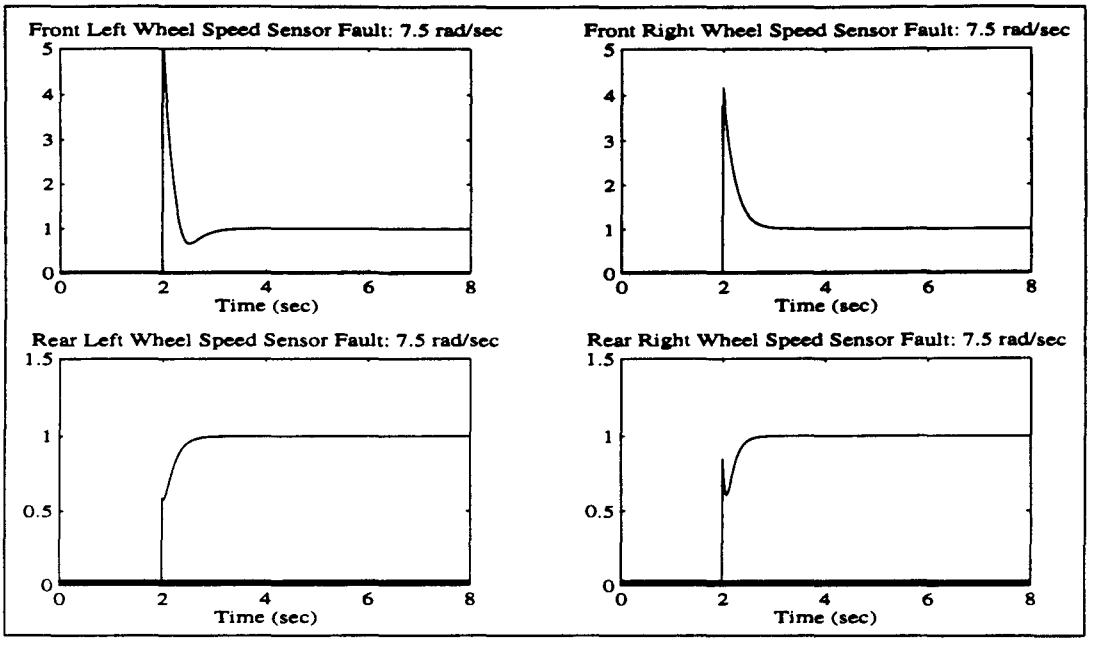

Figure 5.3: Residuals for fault detection filter three.

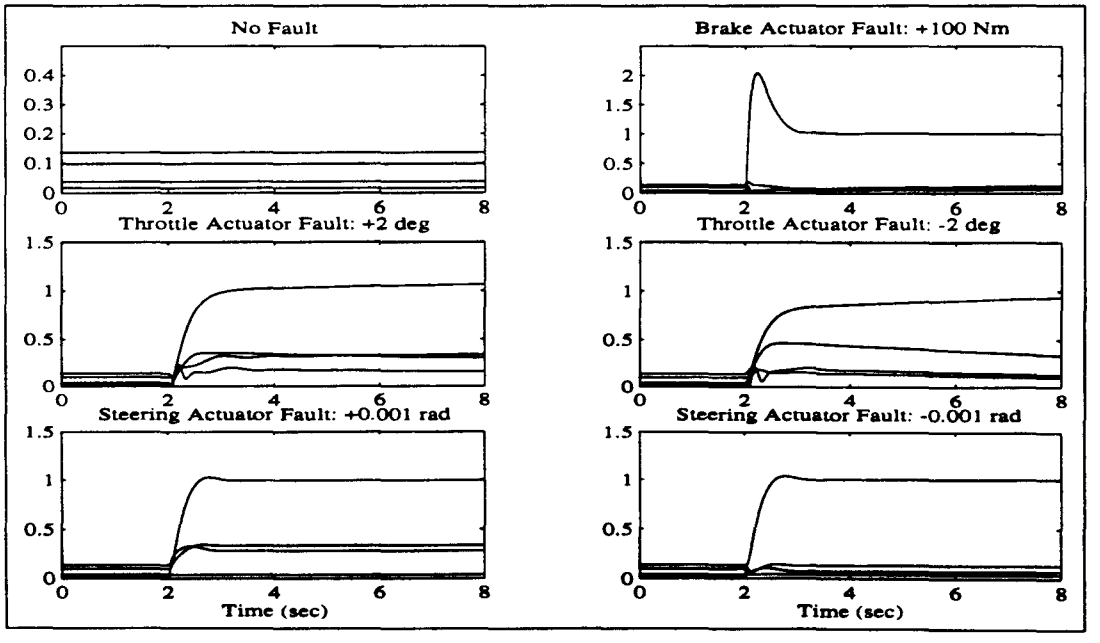

Figure 5.4: Residuals for fault detection filter four.

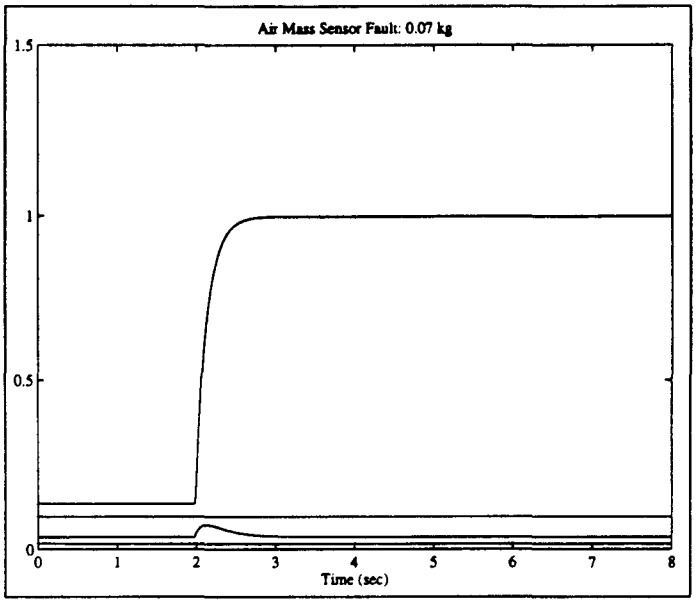

Figure 5.5: Residuals for fault detection filter four.

Figures 5.6 and 5.7 show the residuals for the four fault detection filters derived from the first fault group. Figure 5.6 illustrates a visually obvious contrast between cases where no fault occurs and where a step fault does occur in the engine speed sensor and lateral accelerometer residuals. In Figure 5.7, bias faults in either the pitch rate sensor or the vertical accelerometer are only barely visually detectable. The reason is the the nominal bias fault size is dominated by the noise produced by the rough road model. In the case of the vertical accelerometer, the noise standard deviation is about $0.3\frac{m}{sec^2}$ while the nominal bias fault size is $0.1\frac{m}{sec^2}$. While the fault may not be visually detectable, both residual processing systems, the Bayesian neural network of Section 6 and the Shiryayev sequential probability ratio test of Section 7, quickly and unambiguously detect the fault.

Figures 5.8 and 5.9 show the the residuals for the four fault detection filters derived from the second sensor fault group. Figures 5.10 and 5.11 show the the residuals for the four reduced-order fault detection filters derived from the third sensor fault group.

Analysis is more difficult for the residuals produced by the fault group four detection filter. The actuator faults in this group stimulate the nonlinear vehicle dynamics, alter the

operating point and cause all residuals to respond, not just the residual associated with given fault. Thus all residuals are examined as an actuator fault occurs. Figures 5.12 through 5.18 show that all faults are clearly identifiable and distinguishable from one another.

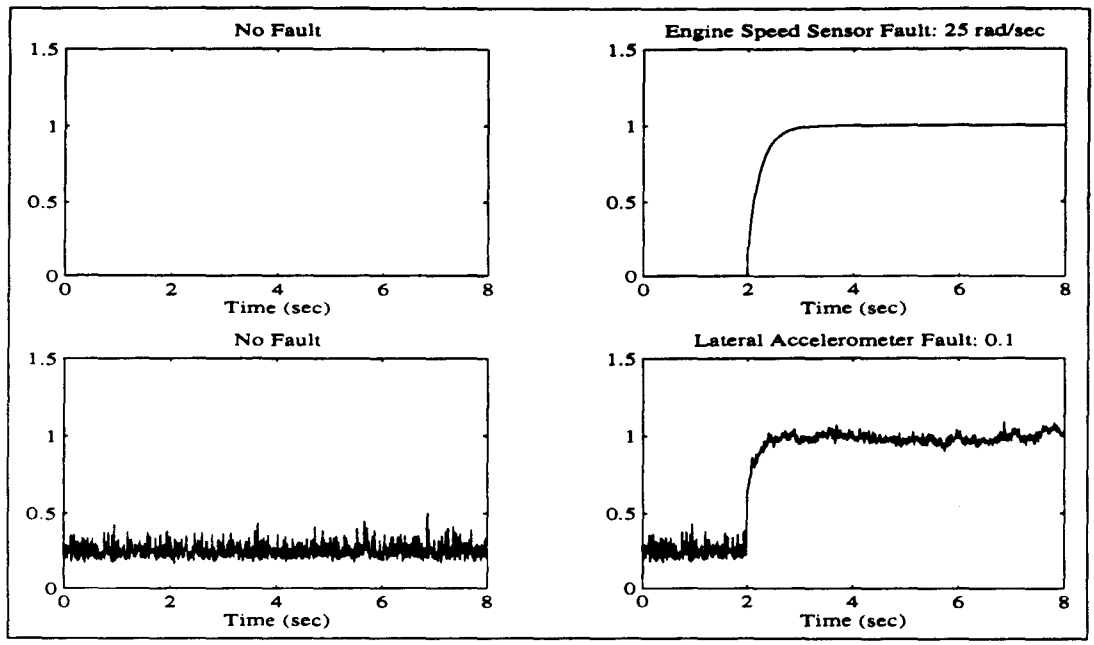

Figure 5.6: Residuals for fault detection filter one.

5.2 Fault Detection Filter Evaluation On A Straight Rough Road

In this section, the performance of a longitudinal mode fault detection filter described in (Douglas et al. 1995) is evaluated for robustness to noise caused by rough roads. The same types and sizes of faults are used here as in (Douglas et al. 1995). Figures 5.19, 5.20 and 5.21 illustrate detection filter performance for the first, second and third fault groups Because the rough road noise dominates the nominal vertical accelerometer bias fault, this fault is hard to detect by inspection of the residual. However, both residual processing systems, the Bayesian neural network of Section 6 and the Shiryayev sequential probability ratio test of Section 7, quickly and unambiguously detect the fault.

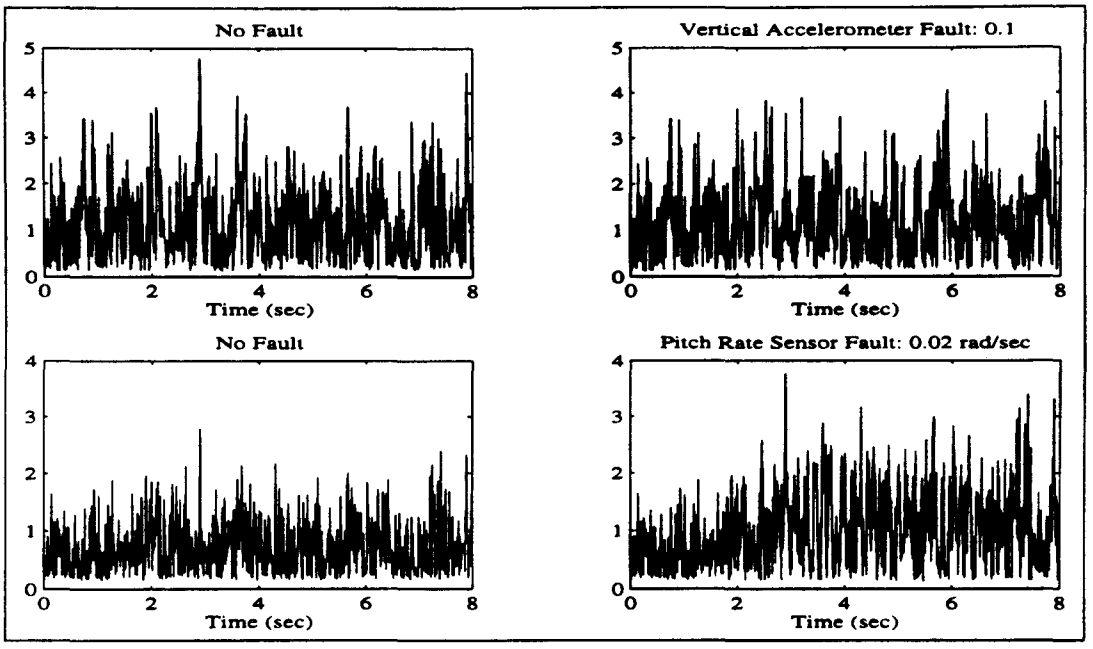

Figure 5.7: Residuals for fault detection filter one.

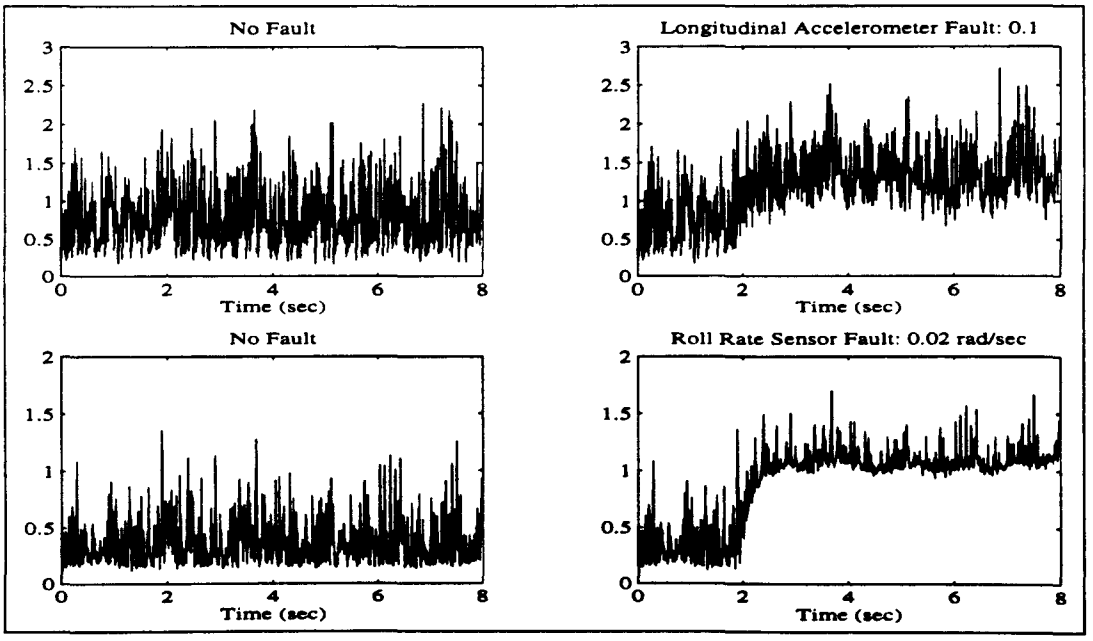

Figure 5.8: Residuals for fault detection filter two.

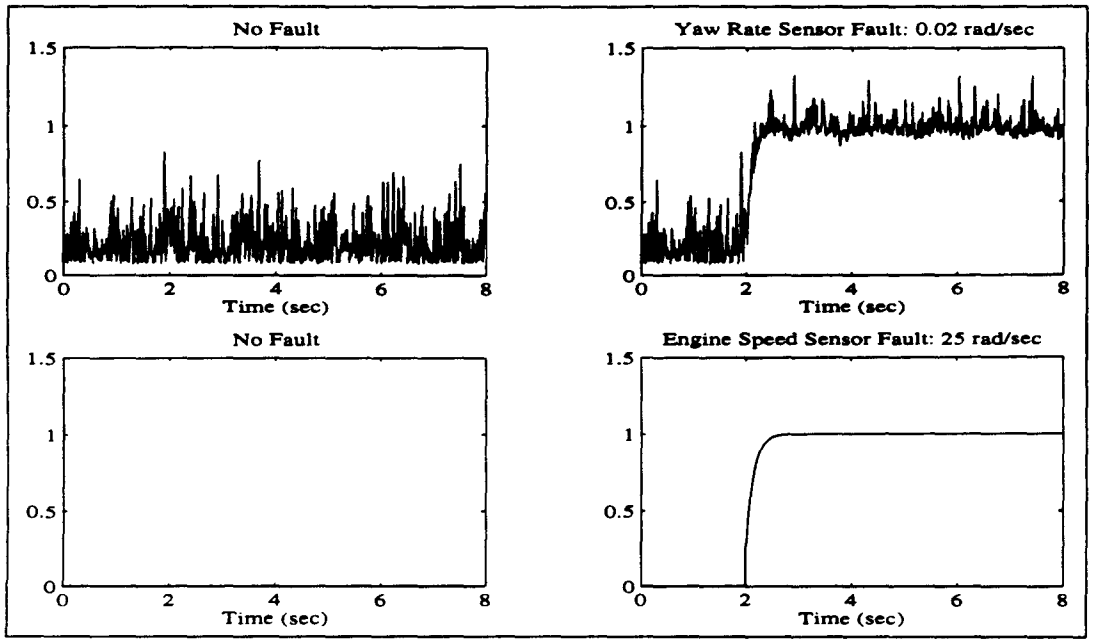

Figure 5.9: Residuals for fault detection filter two.

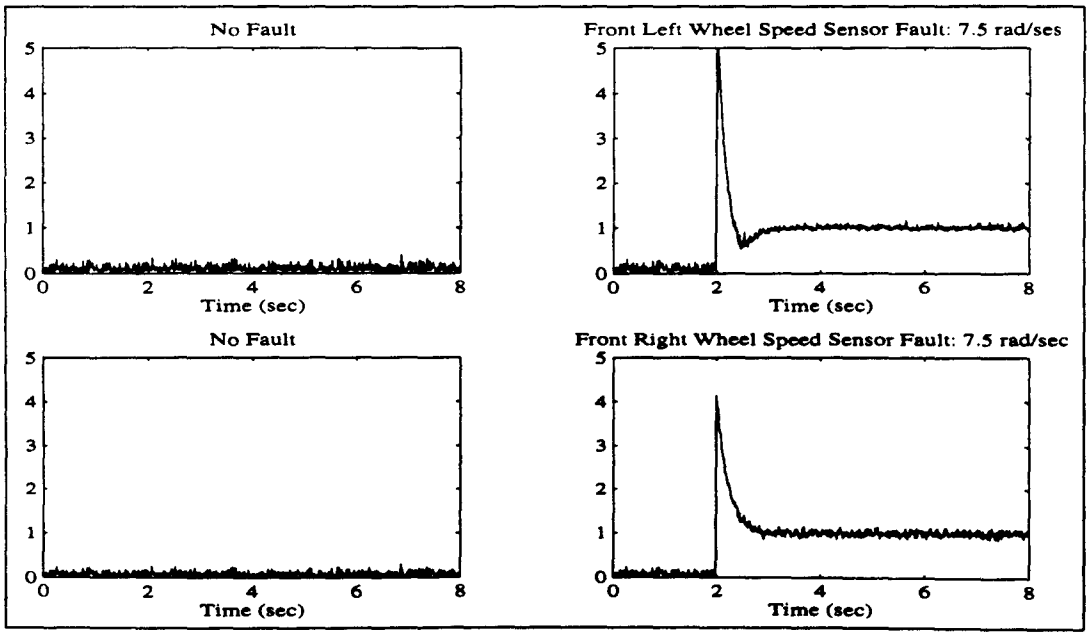

Figure 5.10: Residuals for fault detection filter three.

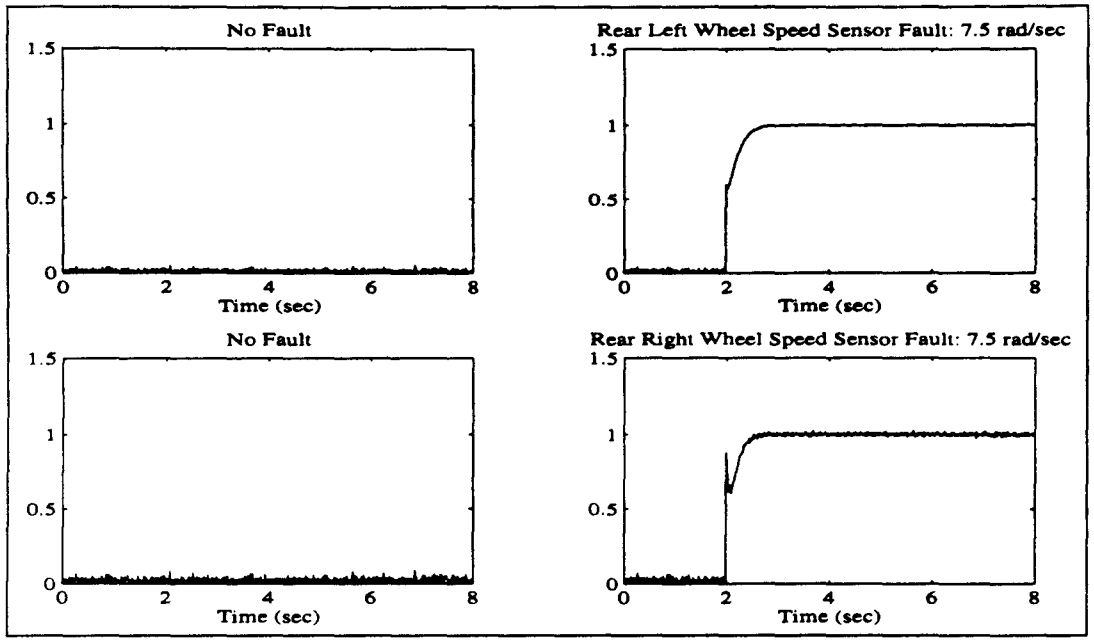

Figure 5.11: Residuals for fault detection filter three.

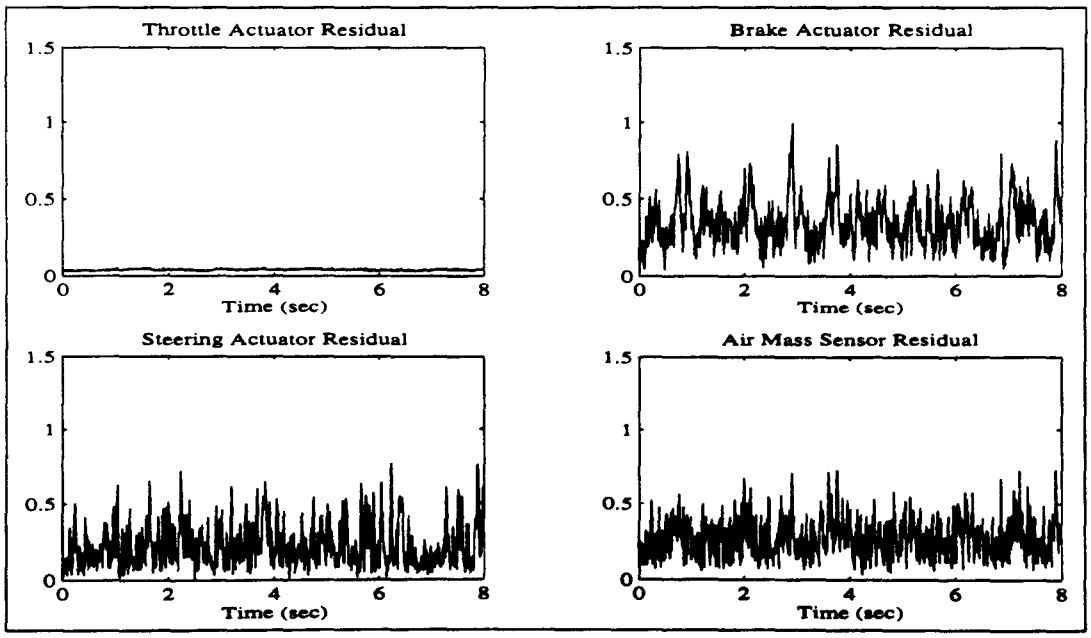

Figure 5.12: Residuals for fault detection filter four, no fault.

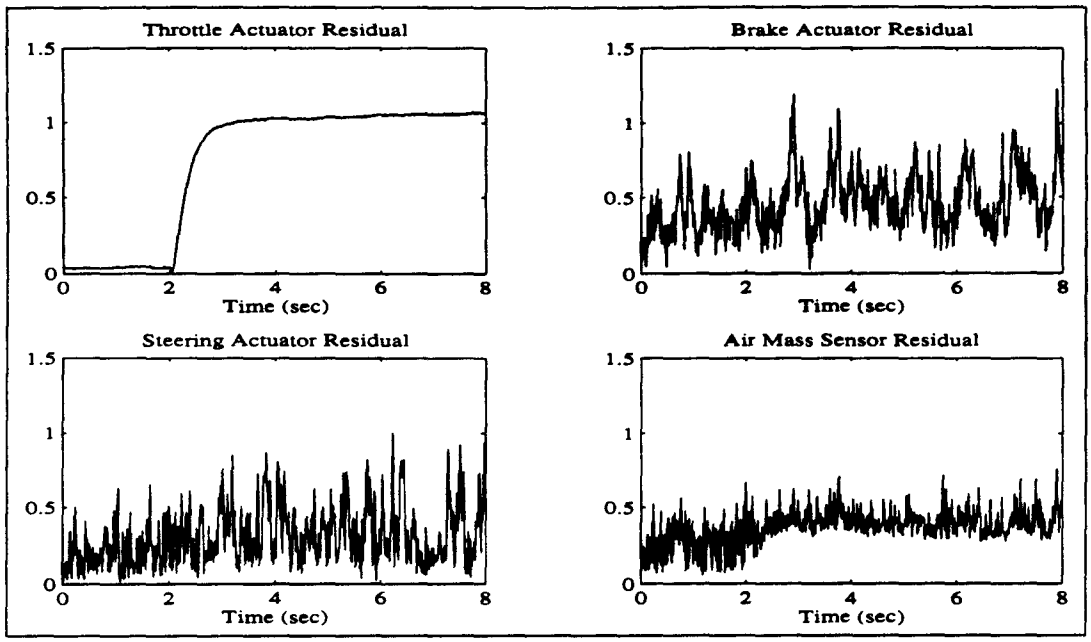

Figure 5.13: Residuals for fault detection filter four, throttle actuator fault +2 deg.

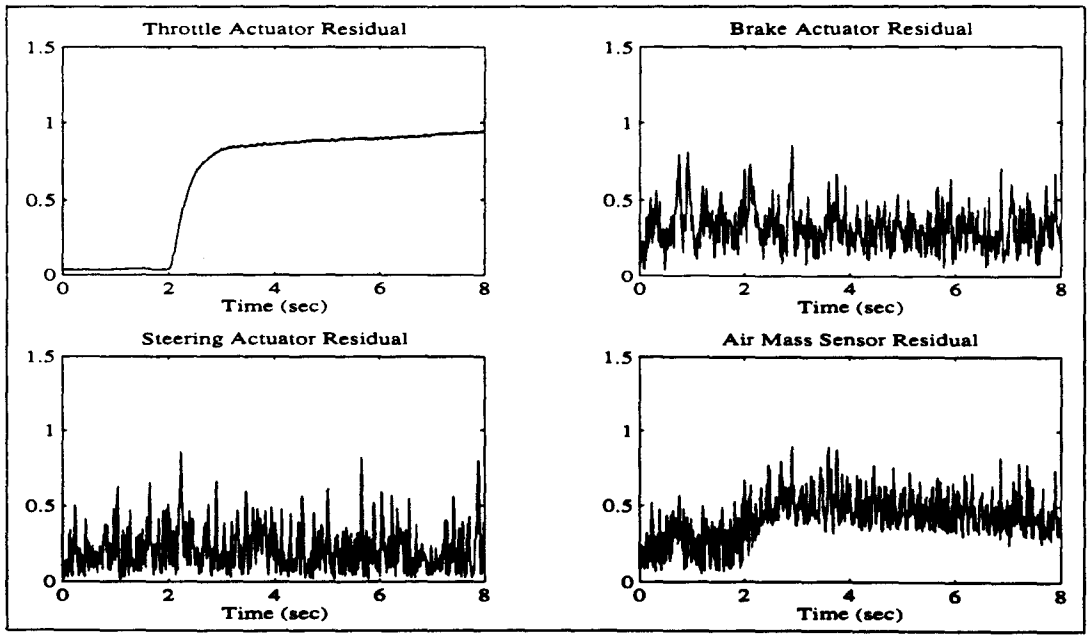

Figure 5.14: Residuals for fault detection filter four, throttle actuator fault -2 deg.

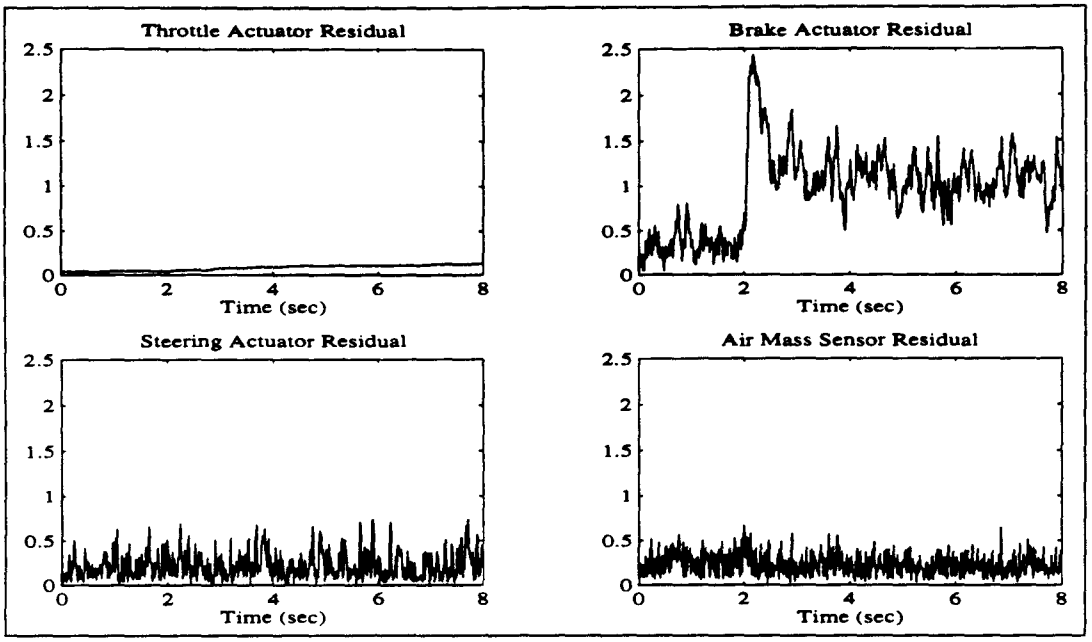

Figure 5.15: Residuals for fault detection filter four, brake actuator fault +100 Nm.

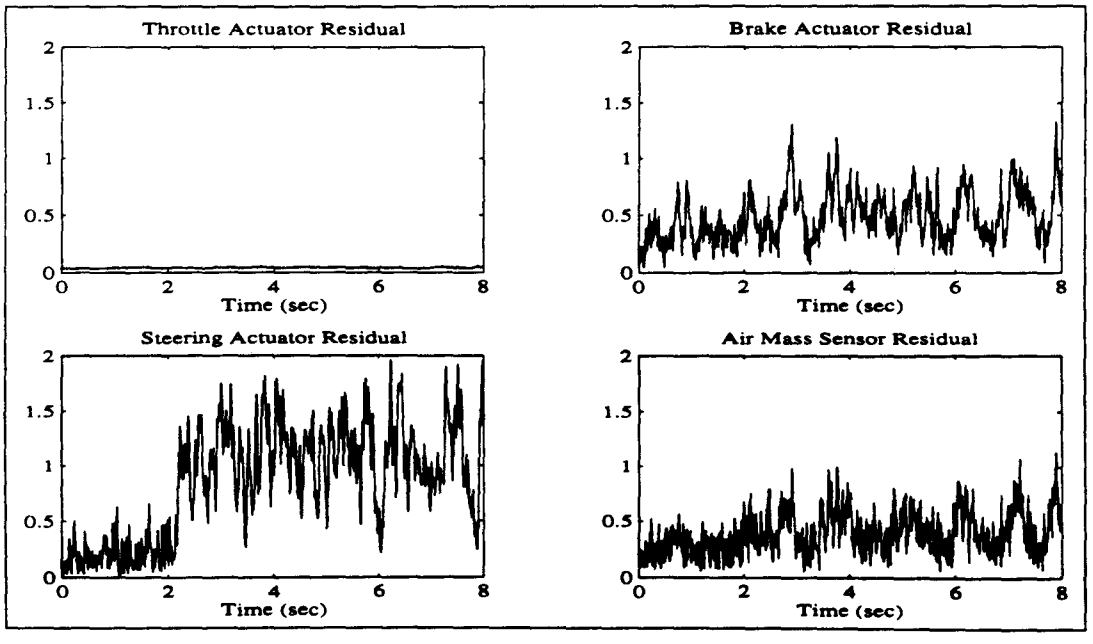

Figure 5.16: Residuals for fault detection filter four, steering actuator fault +0.001 rad.

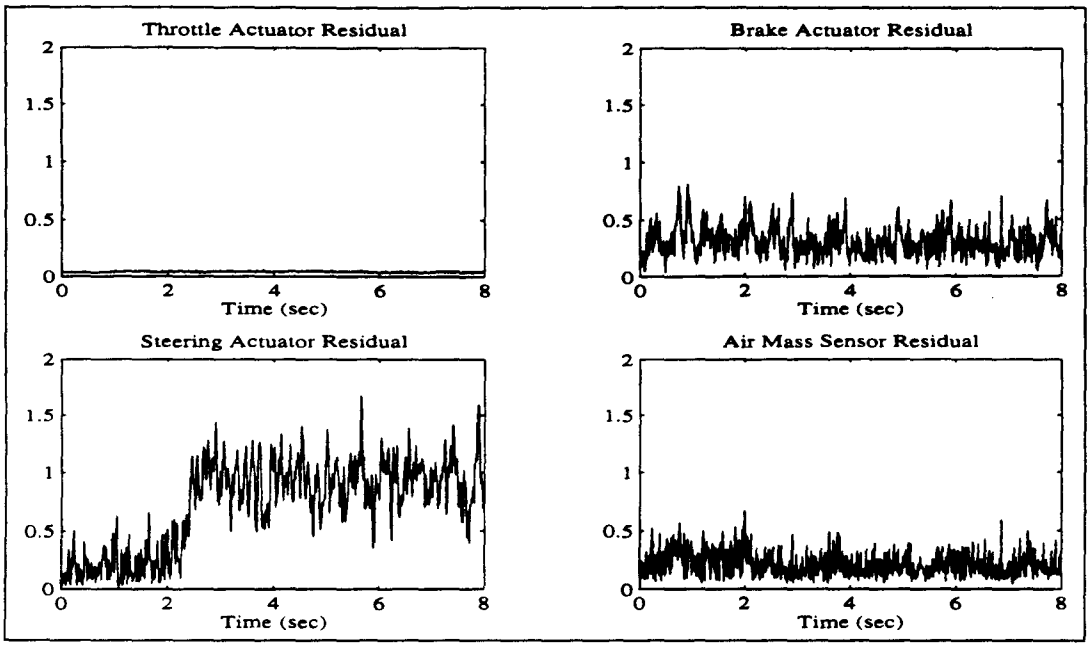

Figure 5.17: Residuals for fault detection filter four, steering actuator fault -0.001 rad.

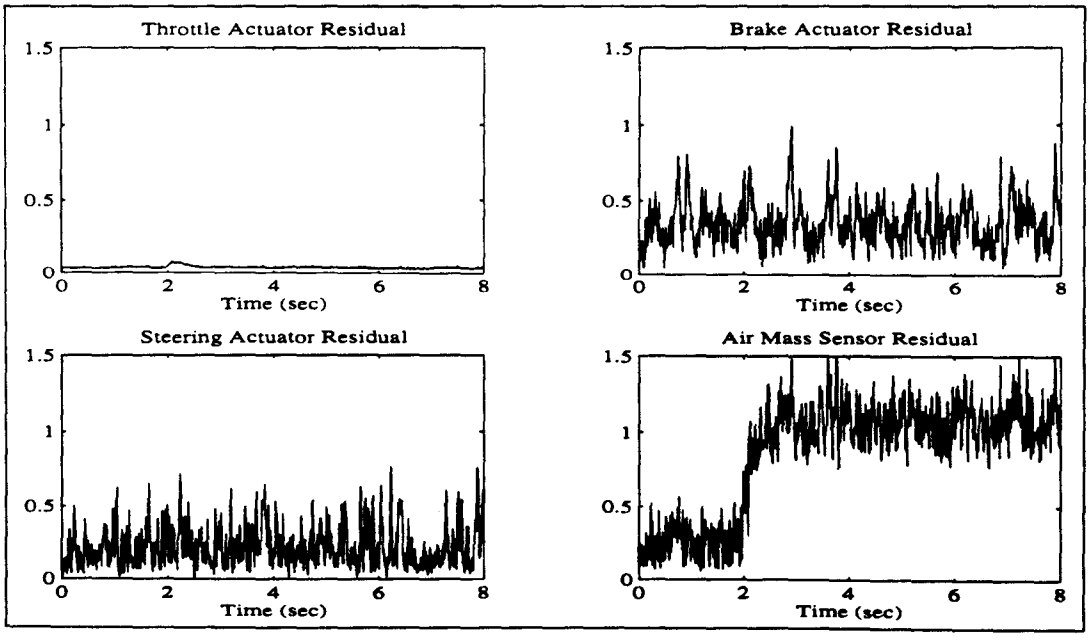

Figure 5.18: Residuals for fault detection filter four, air mass sensor fault 0.07 kg.

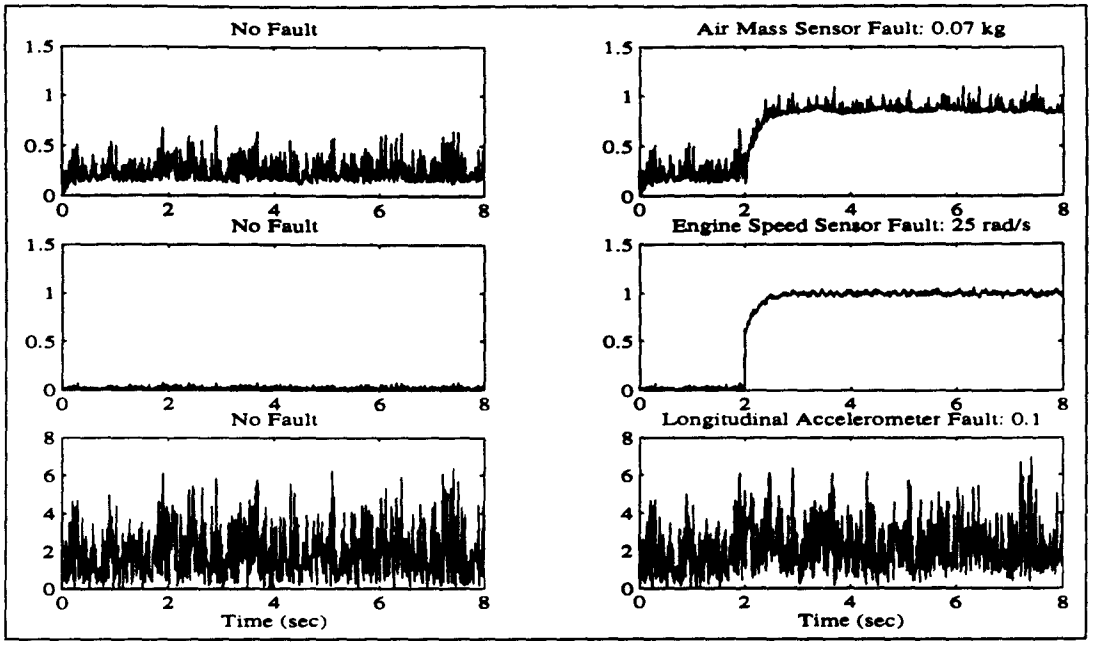

Figure 5.19: Residuals for fault detection filter one: air mass sensor, engine speed sensor and forward accelerometer.

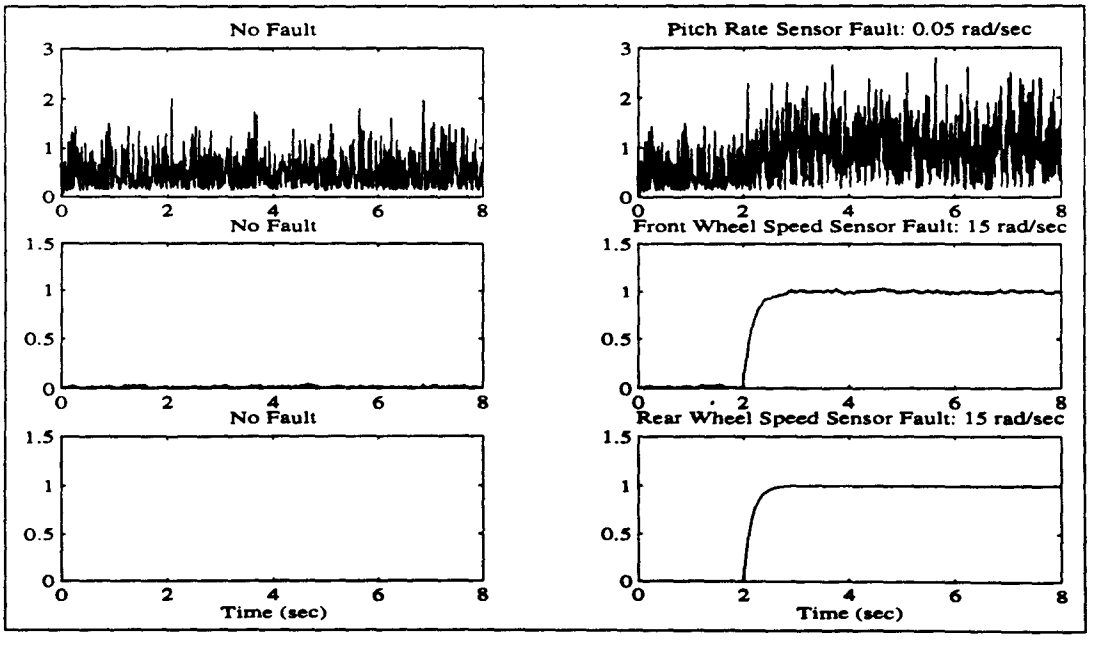

Figure 5.20: Residuals for fault detection filter two: pitch rate sensor, forward wheel speed sensor and rear wheel speed sensor.

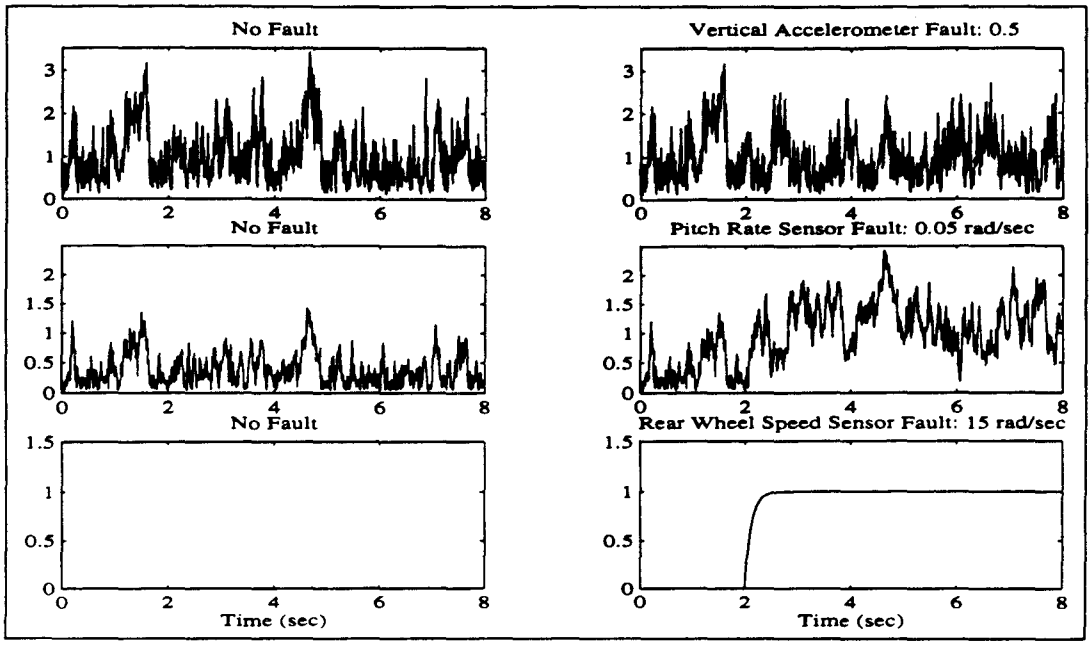

Figure 5.21: Residuals for fault detection filter three: vertical accelerometer, pitch rate sensor and rear wheel speed sensor.

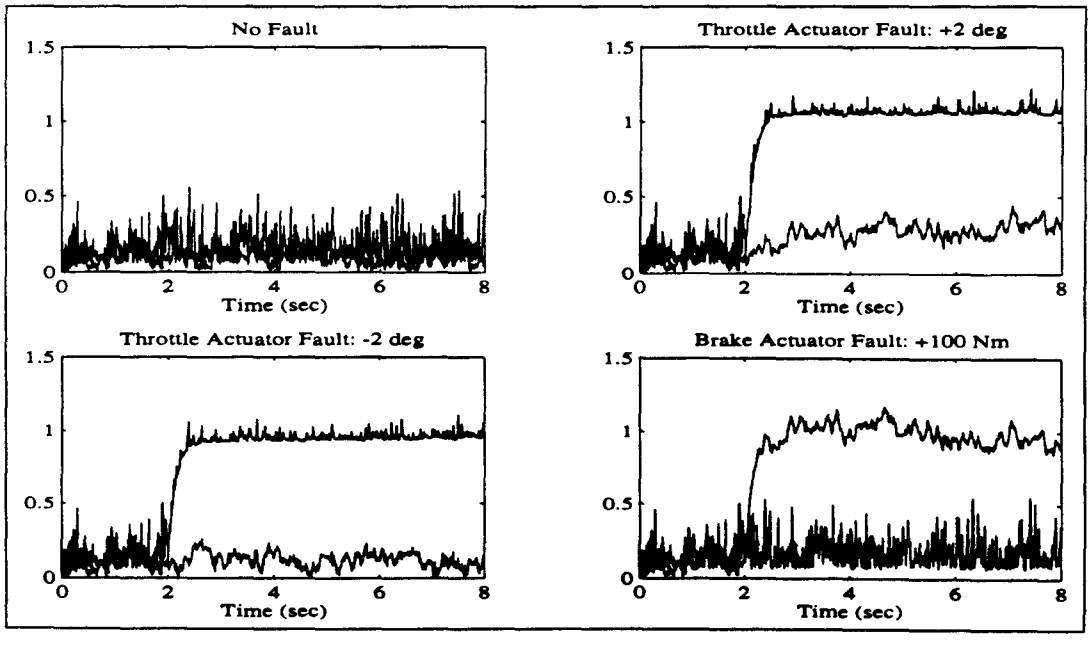

Figure 5.22: Residuals for fault detection filter four: throttle actuator and brake actuator.